Eng Int Syst (2023) 5: 369–378

Engineering
Intelligent Systems

Embedded Inkjet Detection Based on a Convolutional Neural Network

Chenye Han[1]* **and Baojing Liu**[2]*

[1] *School of Networks and Communications, Hebei Polytechnic Institute, Shijiazhuang 050091, China*
[2] *Information Technology and Cultural Management Institute, Hebei Institute of Communications, Shijiazhuang 051430, China*

In a high-speed production line, due to the large number of products and other factors, the inkjet printing of information about the product is easily lost or blurred. To ensure the integrity of inkjet information and eliminate non-acceptable products, an embedded inkjet detection model based on improved CNN is studied and constructed. YOLOv5s algorithm is used to locate the inkjet character area. In the course of research, it was found that the positioning algorithm still has problems such as low accuracy and slow reasoning speed. Therefore, an ECA attention mechanism and CIOU loss function are introduced to improve the algorithm. Then a convolution neural network combined with a cyclic neural network and CTC algorithm is used to recognize inkjet characters. It can timely detect missing information, ambiguity and other defects in the inkjet code. According to the experiment, the average defect detection accuracy of the model is 97.56%, the Re value is 98.56%, and the running time is 26.25ms, which can achieve efficient and accurate inkjet-defect detection. The model provides a technical guarantee for industrial production quality inspection and has positive implications for the development of industrial production enterprises.

Keywords: convolution neural network; inkjet detection; character recognition; attention mechanism

Introduction

Nowadays, consumers pay more attention to the quality and safety of food, medicine and other edible goods. Production date, shelf life, etc. are important criteria enabling consumers to determine product quality when purchasing goods [1]. Because the products with inkjet characters usually have complex background colors, the different inkjet styles used to print information and the outer packaging often have similar non-inkjet produced fonts, which increases the difficulty of detecting inkjet characters. The machine vision-inspection function has greatly improved the quality inspection of commodity production [2]. Inkjet defects may affect the pass rate, reduce production efficiency and even cause food safety issues. The existing inkjet detection equipment has a high recognition rate for defects such as missing inkjet and wrong positioning, but it is often unable to achieve ideal recognition results for defects such as unclear characters and incomplete fonts [3]. Deep learning algorithms have been widely used for image processing and other tasks [4]. The convolution neural network (CNN) is a feedforward neural network with strong structure and convolution computation. It imitates the construction of the biological visual perception mechanism and can conduct supervised learning and unsupervised learning [5]. In order to ensure the integrity and clarity of the inkjet information on products flowing into the market, the improved YOLOv5s and improved convolutional recurrent neural network (CRNN) are studied to detect the defects of the inkjet information on a product's packaging. Therefore, an embedded inkjet detection model based on improved CNN is constructed, which is applied to industrial production lines to ensure that there is less loss of commodity production information.

*Email of corresponding authors: Chenye Han: hanchenye19841230@163.com, Baojing Liu: myyangguang73@163.com

1. RELATED WORKS

CNN imitates the cognitive structure of the human brain for processing information, and consists of multiple neurons. The connection between different neurons is complex. The application and improvement of CNN has also become the focus of research. Djenouri et al. [6] collected vehicle data and used a SIFT extractor to remove noise, and then used regional CNN to detect vehicles. To improve CNN, a hyperparametric optimization model is used to adjust the parameters of the framework. Yin et al. [7] integrated the heterogeneous data of T2 MRI images and clinical data into CNN to diagnose Parkinson's disease. They applied the Gabor filter to CNN to improve the algorithm. Jiang et al. [8] proposed a weld defect identification method based on CNN to solve the problems of poor dynamic adaptability of pool strategy and insufficient feature selection ability in weld defect identification. The ReliefF algorithm pair was introduced to improve CNN. To effectively solve the overlapping in images of fundus lesions, Ding et al. [9] used the effective search ability of the shuffle frog jump algorithm to optimize the weight initialization and back propagation of CNN. A single-population hop-optimized CNN algorithm is constructed to detect and classify various fundus lesions. Wang et al. [10] constructed a new feature fusion structure based on the improved U-Net CNN. This fusion feature structure further refines the features at different semantic levels and improves the accuracy of sea ice detection. Guo et al. [11] proposed an improved deep CNN network with dual channel parallel input in the time domain and frequency domain to detect the degradation process and predict the residual service life of rolling bearings.

As the last link in the production line, the Not sure whether I have interpreted this correctly. on product packaging plays a particularly important role. Currently, more research is being conducted on character detection. To study Tibetan historical documents and solve the problem of character segmentation in the documents, Zhang et al. [12] shortened the text line using projection and syllable point position information, and divided the character block into two regions using different segmentation methods, which achieved good segmentation results and provided a reference for the segmentation of characters in a document. Akin Sherly and Jaya [13] proposed an improved algorithm for firefly local capture using CNN feature extraction. In the process of feature extraction, the method is used to adjust the super parameters of CNN to recognize characters from multi-scene images. For an accurate automatic license plate recognition system, Alghyaline [14] used two-level CNN based on YOLOv3 framework, and uses time information from different frames to remove false predictions. The experimental results show that the recognition accuracy of the proposed system reaches 87%. To achieve multi-scale Chinese character detection and location, Kim and Choi [15] used convolution filters of different sizes and fully-connected networks. Compared with the single-scale faster R-CNN method, the accuracy is improved by 3%. Zabaldo and Ueda [16] used the automatic simulation of a genetic algorithm to study the problem that the camera will capture a blurred image during motion, resulting in information loss. The recognition score after optimizing the camera track reaches 65%. To summarize the research progress of document character recognition and propose the research direction, Memon et al. [17] collected 176 articles (from 2000 to 2019) related to optical recognition of handwritten character. Their research conclusions provided a new direction for subsequent research.

The literature revealed that there are many studies on character recognition methods, but there are few studies on the application of CNN to inkjet detection. To ensure the integrity of inkjet-generated information and eliminate unacceptable products, an embedded inkjet detection model based on improved CNN is studied and constructed. This research provides a technical guarantee for the production quality of a commodity production line.

2. CONSTRUCTION OF EMBEDDED INKJET DETECTION MODEL BASED ON IMPROVED CNN

2.1 Inkjet Character Location Based on Improved YOLOv5s

Character positioning is used to determine the area where the inkjet characters will be located in the commodity image, which is the front-end task of inkjet character recognition. The positioning directly affects the system's character recognition [18]. The general steps of the traditional character location algorithm are: 1) preprocess the image; and 2) manually design the feature extraction target. This method has poor robustness when the background environment is complex. YOLOv5 algorithm is selected to locate the inkjet target. YOLOv5 network uses Mosaic data enhancement at the input end, and combines four pictures of the training set into a new training picture by means of shorthand scaling and splicing. The YOLO v5 network structure consists of three parts as shown in Figure 1. The backbone network extracts high-dimensional feature information of images. The neck fuses the feature information of different dimensions of the image. The head is the prediction output layer.

YOLOv5 obtains four network models through parameter control. The research selects YOLOv5s as the character positioning network. Although the detection speed is fast and the model size is small, the detection rate is not high as a front-end task of recognition. To improve its detection performance, the attention mechanism is studied to improve the feature extraction ability of the network. According to the small scale and periodicity of dot inkjet characters, and the real-time algorithm reasoning, the lightweight channel attention module ECA-Net is selected. ECA-Net involves only a small number of parameters, which can maintain high detection performance while reducing complexity, avoid reduction of feature dimension and increase information interaction between channels. There are two steps in the weight calculation process of ECA-Net. Firstly, the feature map is pooled globally and the vector is generated. Then, the information interaction between channels is completed

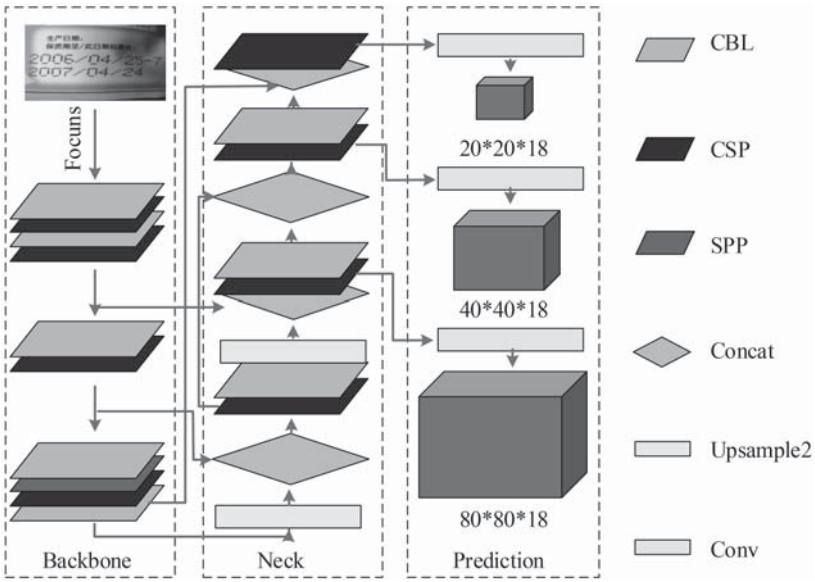

Figure 1 Schematic diagram of YOLOv5 network structure.

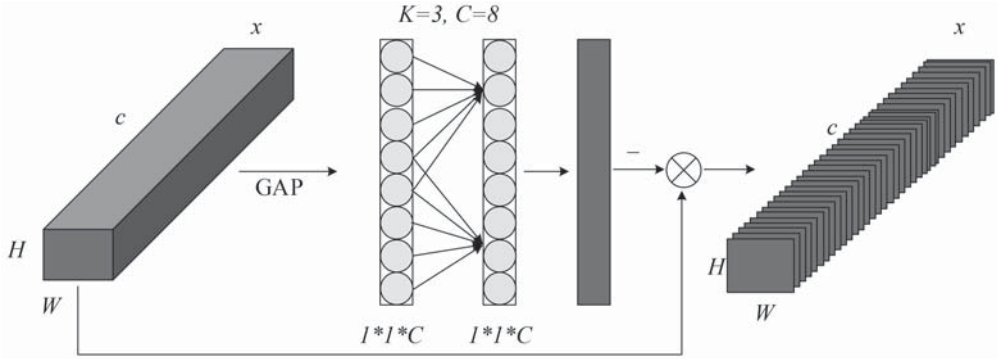

Figure 2 Schematic diagram of ECA attention module.

through one-dimensional convolution, and the weight of each channel is obtained. Formula (1) is used to calculate the weight.

$$w_i = \sigma\left(\sum_{j=1}^{k} w_i^j y_i^j\right), y_i^j \epsilon \Omega_i^k \tag{1}$$

In Formula (1), σ is the sigmoid activation function. w_i is the weight of channel characteristic y_i. w_i^j is the channel attention learned. Ω_i^k is the collection of k adjacent channels of channel characteristics. The research uses a one-dimensional convolution to achieve information interaction between channels, as shown in Formula (2).

$$w = \sigma(ConvID(y)) \tag{2}$$

In Formula (2), $ConvID$ is a one-dimensional convolution, which involves k parameter information. The amount of parameter information is proportional to the channel dimension, as shown in Formula (3).

$$C = \phi(k) = 2^{(y*k-b)} \tag{3}$$

After the channel dimension is determined by Formula (3), the convolution kernel size is calculated using Formula (4).

$$k = \left|\frac{\log_2(C) + b}{\gamma}\right|_{odd} \tag{4}$$

In Formula (4), $|x|_{odd}$ represents the nearest odd number. γ and b are constant coefficients. The structure of the ECA channel attention module is shown in Figure 2.

The loss function of the target detection task usually consists of classification loss, confidence loss and prediction rectangle loss. And their category score, confidence score and rectangular box score of the prediction result are calculated in sequence. YOLOv5 uses a combination of binary cross entropy (BCE) loss function and sigmoid to transform the multi-label classification problem into a two-classification problem for each label to avoid gradient dispersion and other problems during network training. Formula (5) shows the calculation.

$$BCE(c_i, (\hat{c}_i)) = -\hat{c}_i \times \log(c_i) - (1 - \hat{c}_i) \times \log(1 - \hat{c}_i) \tag{5}$$

From Formula (5), the class prediction loss of the positive sample of the network classification loss function is obtained as Formula (6).

$$lcls = \sum_{i=0}^{s^2} 1_{ij}^{obj} \sum_{c \epsilon classes} [\hat{p}_i(c) \log(p_i(c)) + (1 - \hat{p}_i(c)) \log(1 - p_i(c))] \tag{6}$$

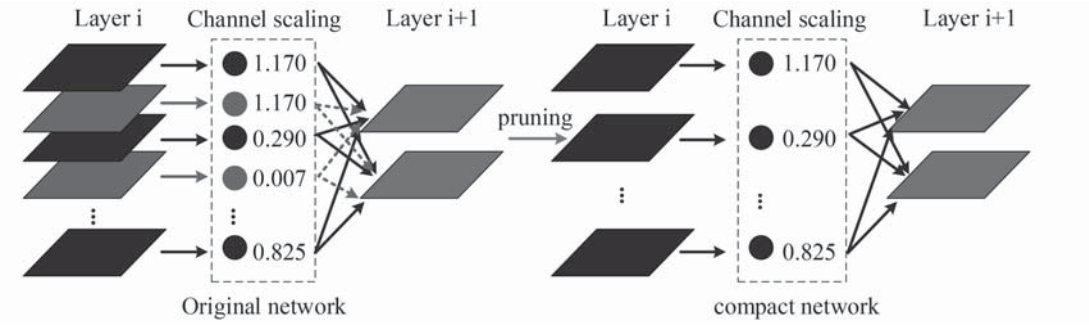

Figure 3 YOLOv5s network model pruning and compression process.

In Formula (6), s^2 is the characteristic layer of three different scales. 1_{ij}^{obj} Indicates whether the target is included at i and j. If there is a target, the value is 1. Formula (7) is used to calculate the the amount of confidence loss.

$$lobj = \sum_{i=0}^{s^2}\sum_{j=0}^{B} 1_{ij}^{obj}[\hat{C}_i \log(\hat{C}_i) + (1-\hat{C}_i)\log(1-C_i)] - \lambda_{noobj}\sum_{i=0}^{s^2}\sum_{j=0}^{B} 1_{ij}^{obj}[\hat{C}_i \log(\hat{C}_i) + (1-\hat{C}_i)\log(1-C_i)] \tag{7}$$

In Formula (7), B is the number of bounding boxes. λ_{noobj} is a super parameter used to adjust the proportion of the execution loss of negative samples. The rectangular frame loss calculates the deviation between the predicted frame and the real frame, and then carries out back-propagation training to optimize the network parameters. The GIoU loss function is used for the rectangular box loss of YOLOv5. However, the study found that the GIoU loss function could not be regressed and the network convergence speed slowed down when the labeled real frame completely surrounded the prediction frame. Therefore, the CIoU loss function is used to calculate the regression loss of the boundary box, as shown in Formula (8).

$$\begin{cases} L_{CIOU} = 1 - IoU + \frac{||b^{pre}-b^{gt}||_2^2}{c^2} + \alpha\nu \\ \nu = \frac{4}{\pi^2}\left(\arctan\frac{w^{gt}}{h^{gt}} - \arctan\frac{w}{h}\right)^2 \\ \alpha = \frac{\nu}{(1-IoU)+\nu} \end{cases} \tag{8}$$

In Formula (8), IoU is the intersection and combination ratio of the real frame and the prediction frame. b^{pre} is the central punctuation of the prediction box. b^{gt} is the center punctuation of the real frame. c is the diagonal distance containing the predicted and actual minimum rectangle C. ν is the introduced aspect ratio factor. The results of Formulas (6)-(8) are summed to obtain the final loss function: Formula (9).

$$Loss = lcls + lobj + L_{CIoU} \tag{9}$$

YOLOv5s is an excellent lightweight detection network. However, for the embedded end, the model is still large, which takes up a large storage space, resulting in an increase in the amount of computation and a slow reasoning speed. Therefore, the YOLOv5s network model needs to be pruned and compressed, and its network structure and parameters are trimmed. The sparse pruning method based on convolution kernel parameters is given. The L1 regular term is included in the loss function to constrain the batch normalization (BN) layer coefficient, and the training coefficient is sparse, which results in more convolution kernel parameter values being distributed around "0". The parameters with smaller weight values in this layer are trimmed, and then after pruning, the model is obtained through iteration. The pruning process is shown in Figure 3.

BN layer standardizes data, as shown in Formula (10).

$$\hat{x}_i = \frac{x_i - \mu_B}{\sqrt{\sigma_B^2 + \epsilon}} \tag{10}$$

In Formula (10), μ_B is the mean value of channels and σ_B^2 is the variance. x is the input data vector. m is the batch size. The value of ϵ is 10–3, which prevents the denominator variance is 0. To enhance the ability of network expression, the adjustment of data distribution is studied, and the adjustment method is shown in Formula (11).

$$y_i = \gamma\hat{x}_i + \beta \tag{11}$$

In Formula (11), y_i is the final output of BN layer. γ and β are adjustment parameters learned through network training. Based on the above contents, the YOLOv5s algorithm is studied to detect the location of inkjet characters, and the algorithm is improved to provide a prerequisite for character recognition.

2.2 Embedded Inkjet Character Recognition Based on CRNN

Dot inkjet printing is a portable and fast inkjet printing method. However, during the actual production, due to the large number of products, close spacing, random placement and mechanical vibration of the inkjet printer itself, the inkjet-produced information may be lost [19]. To detect the inkjet code on the product's packaging and ensure the integrity of the inkjet printing on the commodities flowing into the market, the research uses the CNN algorithm to build the inkjet code detection and recognition model. After obtaining the location area of the inkjet code through the previous content, in order to recognize and analyse the character pictures with different lengths, the CNN and cyclic neural network (RNN) are

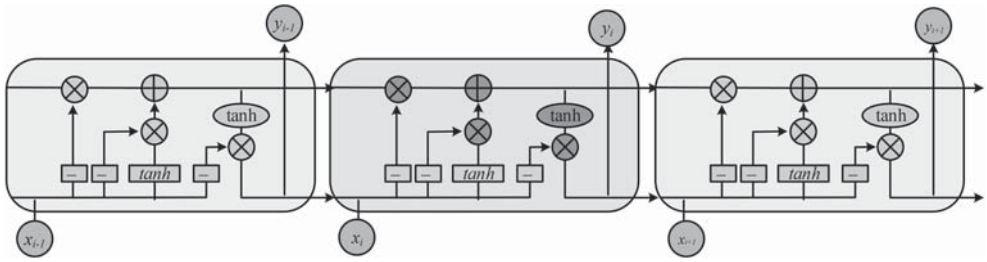

Figure 4 LSTM network structure.

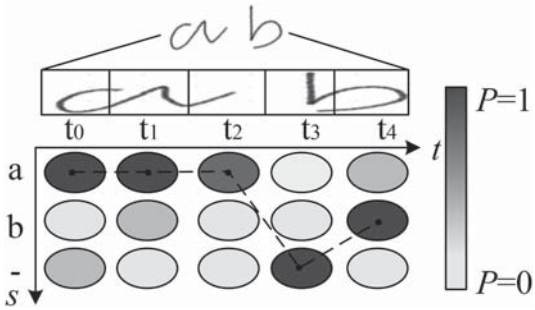

Figure 5 Character sequence correspondence mechanism of CRNN network calculation.

combined to form the CRNN algorithm. In this research, CNN is used to extract image feature information, and then RNN is used to extract sequence features between character contexts and, finally, the connection time series classification (CTC) algorithm is used to calculate the loss in training. RNN uses a bidirectional short-term and short-term memory network (LSTM) to extract temporal features, namely the recursive layer. The image features extracted by CNN into LSTM are input to achieve long-sequence character recognition. The LSTM recursion layer is shown in Figure 4.

Each time step of the LSTM output corresponds to one character, so each input image needs to mark the position of each character in the image, but this is difficult to achieve [20]. In general, the input width will be greater than the output sequence length, which leads to redundant information. Corresponding to the character recognition task, a character may be recognized several times in succession. If the operator simply removes the duplicate characters, it cannot be used for the case when the characters originally contained the same characters. Hence, the CTC algorithm is introduced to calculate the loss function, so that the LSTM can be trained and the loss can be calculated without aligning the characters, and the parameters can be updated. The CTC algorithm solves relevant problems by adding a placeholder, and translates the character sequence into the final correct recognition result. The conditional probability of the input sequence is shown in Formula (12).

$$p(\pi|x) = \Pi_{t=1}^{T} y_{\pi_t}^{t} \tag{12}$$

In Formula (12), π represents the path. y_k^t is the probability of the k th tag on the space B at the time of t. Remove all labels with continuous repeating labels and blank placeholders, as shown in Formula (13).

$$f{:}B^T \rightarrow A^{\leq T} \tag{13}$$

In Formula (13), $A^{\leq T}$ is the set of all possible output tag sequences of a given sequence x in the tag space. Because the paths are different, and a tag sequence can correspond to multiple correct paths. The sum of the probabilities of all paths can be expressed by the sum of the conditional distribution probabilities of the tag sequence in the input sequence, as shown in Formula (14).

$$p(l|x) = \sum\nolimits_{\pi=f^{-}1(x)} p(\pi|x) \tag{14}$$

In Formula (14), l is the tag sequence. The corresponding mechanism of character sequence calculated by the CRNN network is shown in Figure 5.

According to the mapping relationship, the research deletes the continuous repeated characters and placeholders, and obtains the correct recognition results. However, multiple characters can be combined into multiple mapping results, so a label can have multiple paths. The forward and backward algorithm is used to calculate the path probability. The loss function in the calculation process is shown in Formula (15).

$$L(S) = -1n\Pi_{(x,z)\epsilon S} p(z|x) = -\sum\nolimits_{(x,z)} 1np(z|x) \tag{15}$$

In Formula (15), S is the training set. z is the label of sequence x. The printing position of inkjet character area is random, which is more complex than the background of scene text recognition. In addition, the types of inkjet character sequences are limited, usually Arabic numerals and special alphabetic symbols can be recognized, and the length is also limited. According to the characteristics of the inkjet characters and the actual requirements of the embedded end, the lightweight processing of CRNN algorithm is studied. In order to ensure the character recognition rate, the network structure is simplified and the reasoning speed is improved. Firstly, the CNN convolution structure of CRNN is lightened. Using a 5×5 convolution kernel at the front of the original network structure, the fill and step size are set to 2 to increase the perception field of the image. After the second layer, add a 1×1 convolution kernel after each convolution layer,

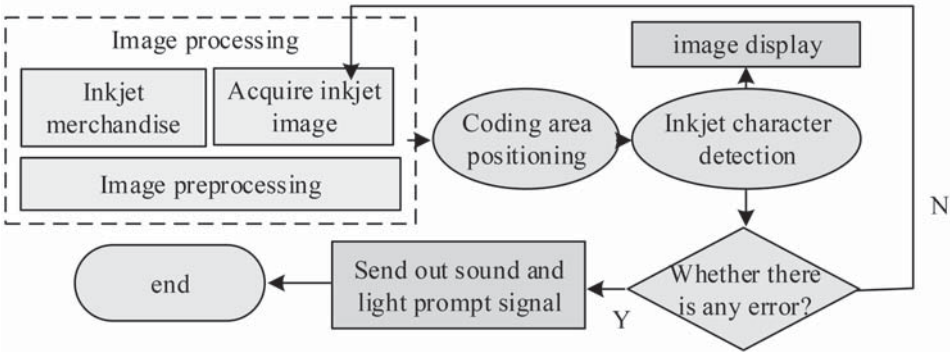

Figure 6 The inkjet error-detection process based on convolutional neural network.

which changes the number of channels in the feature layer. The study uses simple Relu as the activation function. Based on the above operations, the YOLOv5s algorithm is used to locate inkjet characters, and the location algorithm is improved. CNN+RNN+CTC is able to recognize and analyse the inkjet characters. The embedded inkjet-error detection model based on YOLOv5s+CNN+RNN ensures the integrity of the inkjet printing of goods that companies put on the market. The process of inkjet character-error detection is shown in Figure 6.

3. PERFORMANCE ANALYSIS OF EMBEDDED INKJET DETECTION MODEL BASED ON IMPROVED CNN

3.1 Experimental Verification and Analysis of Improved Character Location Algorithm

The loss function of YOLOv5s algorithm is improved, and the rectangular box loss function is changed to CIOU for optimization. To verify the optimization effect of the loss function, the training of character location detection for the improved network is studied by using the test set. The frame regression loss, confidence loss, accuracy rate and positioning accuracy in the training process are recorded, and shown in Figure 7.

In Figure 7, the network loss value gradually decreases as the iterations increase. The detection accuracy and positioning accuracy increase with iterations. The loss curve of the network before and after the improvement in Figure 7 (a) and Figure 7 (b) is basically the same. Both the frame regression loss and the confidence loss reached the final target value after about 140 iterations. As shown in Figure 7 (c), after 60 iterations, the detection accuracy curve of the network model begins to slow down and gradually does not change. At this time, the accuracy rate of the original network is 81%, and the accuracy rate of the improved network is 92%, which is 11% higher than that before the improvement. In Figure 7 (d), the target positioning accuracy was achieved after 160 iterations before showing improvement, and by 27 iterations after improvement, 133 times less than before improvement. According to the content analysis in Figure 7, the convergence speed of the improved network model has not been reduced, and the detection accuracy has increased by 11% compared with that before the improvement, with better positioning of the characters.

This study integrates several improved methods to improve the location algorithm. To further test the fusion improvement effect of the location algorithm, the experiment compares the proposed fusion-improved YOLOv5s algorithm (method 1) with the original YOLOv5s (method 2), YOLOv5s with the ECA attention mechanism (method 3), YOLOv5s with the improved loss function (method 4), and YOLOv5s with the pruning (method 5). Table 1 presents the test results.

In Table 1, the average accuracy of method 2 is 91.27%, the average positioning accuracy is 0.855, and the running time is 25.7 ms. The original network has been added with ECA attention module, namely method 3. Its detection accuracy is 96.63%, which is 5.35% higher than that of method 2. Due to the reduction in the number of missed inspections, the positioning accuracy is reduced by 0.09. The average detection accuracy of method 4 is 96.71%, which is 5.43% higher than that of method 2. The positioning accuracy of method 4 is little different from that of method 2, with a difference of 0.03. The average detection accuracy of method 5 is smaller than that of method 2, and the running time is reduced by 10.72 ms, but the positioning accuracy is reduced by 0.12. The average detection accuracy of method 1 is 98.87%, which is 7.5% higher than the original network, and the positioning accuracy is 0.925, which is 0.16 higher than the original network. Its running time is 17.56 ms, which is 8.14 ms less than that of method 2. According to the comprehensive analysis of the contents in Table 1, the fusion improvement method used in the research has effectively avoided the defects associated with a single improvement method, and has better positioning performance than the original network.

3.2 Performance Analysis of Recognition Algorithm Based on CRNN

The experiment was conducted to compare the performance of the proposed recognition algorithm (algorithm 1) with that of four popular character-recognition algorithms which are: a character recognition algorithm based on BP neural network (algorithm 2), a character recognition algorithm based on SVM (algorithm 3), a character recognition algorithm based on KNN algorithm (algorithm 4), and a recognition algorithm

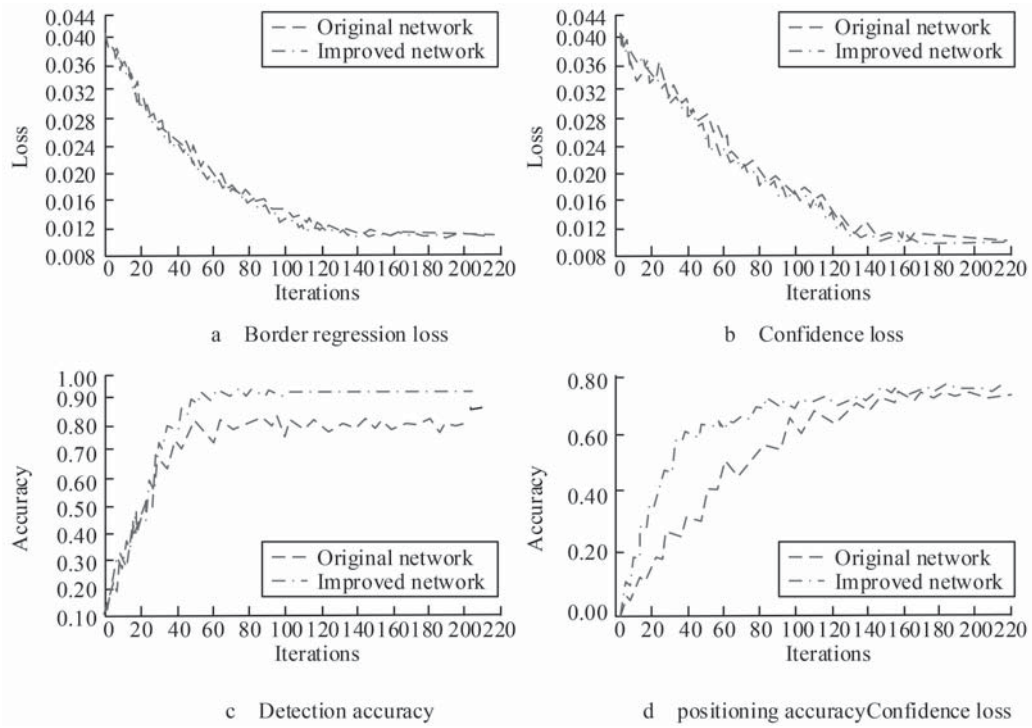

Figure 7 Comparison of training results before and after the improvement of YOLOv5s algorithm.

Table 1 Comparison test results for location algorithm improvement.

	Dataset 1			Dataset 2		
Project	Accuracy (%)	Positioning accuracy (IoU)	Reasoning time (ms)	Accuracy (%)	Positioning accuracy (IoU)	Reasoning time (ms)
Method 1	98.98	0.93	17.65	98.76	0.92	17.47
Method 2	91.48	0.85	25.68	91.26	0.86	25.72
Method 3	96.66	0.76	30.12	96.57	0.77	30.22
Method 4	96.78	0.88	27.46	96.63	0.89	27.83
Method 5	92.36	0.74	14.96	91.98	0.73	15.01

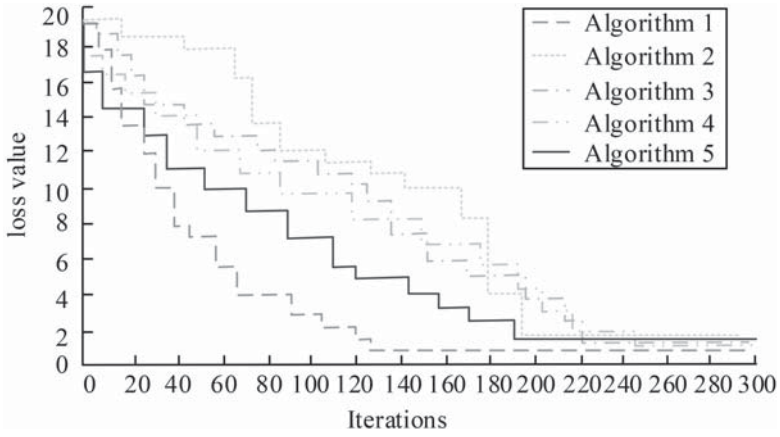

Figure 8 Training iteration changes of each recognition algorithm.

based on LSTM (algorithm 5). The five algorithms are trained. The training results are shown in Figure 8.

As shown in Figure 8, algorithm 1 iterated to 122 times to reach the target loss value. Algorithm 2 iterated to 198 times to reach the target value, 76 times more than algorithm 1. Algorithm 3 iterated to 220 times to reach the target value, 98 times more than algorithm 1. Algorithm 4 iterated to 192 times to reach the target value, 70 times more than algorithm 1. Algorithm 5 iterated to 189 times to reach the target value, 67 times more than algorithm 1. Therefore, algorithm 1 has good convergence.

Table 2 Lightweight network training results.

Method	Accuracy (%)		Model size (M)	Reasoning time (ms)
	Sequence	Character		
CRNN-Full	98.43	98.52	30.28	10.62
No-LSTM	93.25	93.16	21.46	7.51
CNN-Lite	95.46	95.53	10.48	6.48
CRNN-Lite	98.41	98.57	6.31	3.22

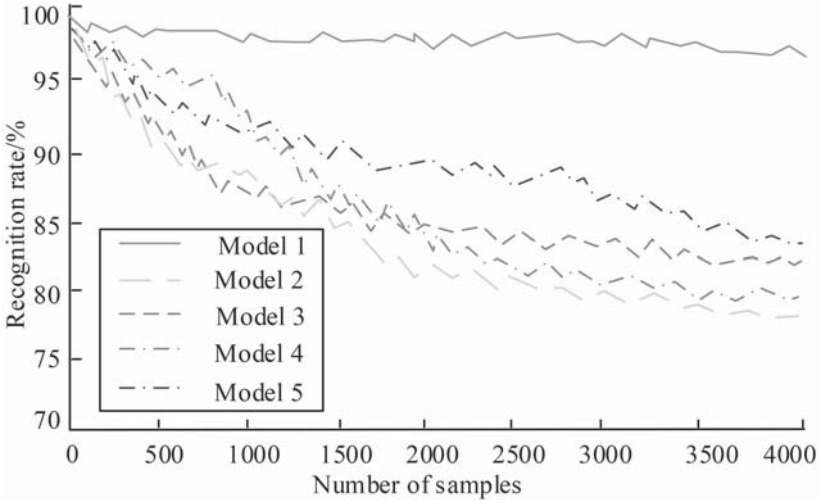

Figure 9 Change curve of detection accuracy with the increase of samples.

To verify the rationality of the lightweight processing of the model, the original CRNN-Full, the improved CRNN-Lite, No-LSTM and lightweight CNN-Lite were trained and tested on the same platform using the same data set. The final training results are presented in Table 2.

The character accuracy rate is 98.57%, which is basically the same as that of the original CRNN-Full. Its running time is 3.22ms, which is 7.40ms less than CRNN-Full. The model size is 6.31M, which is 23.97M smaller than the initial network. As shown in the table, the operation efficiency is significantly improved and the recognition accuracy is always maintained after the lightweight processing of the model.

3.3 Performance Analysis of Inkjet Detection Model Based on Improved CNN

The inkjet defect detection model (model 1) based on improved YOLOv5s+CRNN is compared with several commonly used detection models. The comparison model includes the detection model based on Qt and Arm NN (model 2), the model based on probabilistic neural network (model 3), the detection model based on YOLOv3 and AlexNet (model 4), and the detection model based on LeNet-5+Blob analysis (model 5). In the experiment, five models are used to detect embedded inkjet defects in packaging under the condition of data of different scales. With the increase of the number of samples, the detection accuracy changes as shown in Figure 9.

Figure 9 shows that with the increase of the sample data size, the accuracy of defect identification of the model gradually decreases. The curve change range of model 1 is the lowest, and the accuracy rate is 97.82% when the number of samples is 500. When the number of samples is 4000, the accuracy rate is 96.88%, only reduced by 0.94%. The accuracy of other models decreased by more than 10%. As shown in the figure, model 1 has excellent stability and high defect-recognition accuracy.

Five models are used to detect different defects for further verification of performance. The obtained recall rate (Re), accuracy rate, identification time and other evaluation indicators are shown in Table 3.

In Table 3, the average defect detection accuracy of model 1 is 97.56%, the Re value is 98.56%, and the operation time is 26.25 ms. The accuracy of the other four models decreased by more than 6.31% compared with model 1, the Re value decreased by 6.05% compared with model 1, and the running time increased by more than 5ms. The proposed model can achieve efficient and accurate detection of packaging inkjet defects, and ensure the integrity of inkjet information for goods entering the market.

4. CONCLUSION

The existing inkjet detection equipment has a high recognition rate for defects such as missing inkjet and position errors, but it is often unable to achieve ideal recognition results for defects such as unclear characters and incomplete fonts. To ensure the integrity of the product information flowing into the market and eliminate the unqualified products, the

Table 3 Test results for different defects of the model.

Project		Model 1	Model 2	Model 3	Model 4	Model 5
Vague	Re (%)	98.65	90.46	92.91	85.46	81.47
	Accuracy (%)	97.58	90.25	93.02	85.52	81.48
	Identification time (ms)	26	35	30	40	43
Leaky spray	Re (%)	98.58	90.51	93.02	85.44	81.58
	Accuracy (%)	97.52	90.19	93.21	85.22	80.96
	Identification time (ms)	26	35	31	40	42
Defect	Re (%)	98.49	90.52	92.87	85.49	81.56
	Accuracy (%)	97.53	90.18	93.22	85.23	80.97
	Identification time (ms)	27	36	30	41	42
No defect	Re (%)	98.52	90.57	92.88	85.47	81.48
	Accuracy (%)	97.59	90.19	93.25	85.28	81.22
	Identification time (ms)	26	35	29	39	43

YOLOv5s algorithm is used to locate the inkjet character area, and then the convolutional neural network combined with the cyclic neural network and CTC algorithm are used to recognize the inkjet character. This can timely detect the missing information, ambiguity and other defects in the inkjet. Therefore, an embedded inkjet detection model based on improved CNN is constructed. According to the experimental analysis, the average detection accuracy of the improved YOLOv5s combined with the above improved method 1 is 98.87%. The running time is 17.56 ms, and 8.14 ms lower than the method 2. The average defect detection accuracy of the model built by the research institute is 97.56%, the Re value is 98.56%, and the running time is 26.25 ms. The model can achieve efficient and accurate detection of inkjet defects and provides technical guarantee for the inspection of industrial production quality. To effectively implement the spray printing production line instead of using manual quality inspection, in addition to the detection and identification function, the automatic elimination of unacceptable products can be considered in future research to produce a more comprehensive quality inspection process.

REFERENCES

1. Tay L L, Hulse J. 2021. Methodology for Binary Detection Analysis of Inkjet-Printed Optical Sensors for Chemical Detection. *MRS Advances, 6*(1): 1–5.
2. Henry C, Ahn S Y, Lee S W. 2020. Multinational License Plate Recognition using Generalized Character Sequence Detection. *IEEE Access*, 8: 35185–35199.
3. Galvis J, Morales S, Kasmi C, Vega F. 2021. Denoising of Video Frames Resulting from Video Interface Leakage Using Deep Learning for Efficient Optical Character Recognition. *IEEE Letters on Electromagnetic Compatibility Practice and Applications, 3*(2): 82–86.
4. Sungheetha A, Sharma R. 2021. Design an Early Detection and Classification for Diabetic Retinopathy by Deep Feature Extraction Based Convolution Neural Network. *Journal of Trends in Computer Science and Smart Technology (TCSST), 3*(2): 81–94.
5. Allugunti V R. 2022. A Machine Learning Model for Skin Disease Classification using Convolution Neural Network. *International Journal of Computing, Programming and Database Management, 3*(1): 141–147.
6. Djenouri Y, Belhadi A, Srivastava G, Djenouri D, Chun J, Lin W. 2022. Vehicle Detection using Improved Region Convolution Neural Network for Accident Prevention in Smart Roads. *Pattern Recognition Letters,* 158: 42–47.
7. Yin D, Zhao Y, Wang Y, Zhao W, Hu X. 2020. Auxiliary Diagnosis of Heterogeneous Data of Parkinson's Disease Based on Improved Convolution Neural Network. *Multimedia Tools and Applications*, 79: 24199–24224.
8. Jiang H, Hu Q, Zhi Z, Gao J, Gao Z, Wang R, He S, Li H. 2021. Convolution Neural Network Model with Improved Pooling Strategy and Feature Selection for Weld Defect Recognition. *Welding in the World,* 65: 731–744.
9. Ding W, Sun Y, Ren L, Ju H, Feng Z, Li M. 2020. Multiple Lesions Detection of Fundus Images Based on Convolution Neural Network Algorithm with Improved SFLA. *IEEE Access*, 8: 97618–97631.
10. Wang X, Yang S, Shangguan D, Wang Y. 2022. Sea Ice Detection from SSMI Data Based on an Improved U-Net Convolution Neural Network. *Remote Sensing Letters, 13*(2): 115–125.
11. Guo Y, Zhang H, Xia Z, Dong C, Zhang Z, Zhou Y, Sun H. 2021. An Improved Deep Convolution Neural Network for Predicting the Remaining Useful Life of Rolling Bearings. *Journal of Intelligent & Fuzzy Systems, 40*(3): 5743–5751.
12. Zhang C, Wang W, Liu H, Zhang G, Lin Q. 2022. Character Detection and Segmentation of Historical Uchen Tibetan Documents in Complex Situations. *IEEE Access*, 10: 25376–25391.
13. Akin Sherly L T, Jaya T. 2021. Improved Firefly Algorithm-Based Optimized Convolution Neural Network for Scene Character Recognition. *Signal, Image and Video Processing*, 15: 885–893.
14. Alghyaline S. 2022. Real-Time Jordanian License Plate Recognition using Deep Learning. *Journal of King Saud University - Computer and Information Sciences, 34*(6): 2601–2609.
15. Kim M, Choi H C. Improving Faster R-CNN Framework for Multiscale Chinese Character Detection and Localization. 2020. *IEICE Transactions on Information and Systems, 103*(7): 1777–1781.
16. Zabaldo A, Ueda J. 2021. Camera Trajectory Optimization for Maximizing Optical Character Recognition on Static Scenes with Text. *IFAC-PapersOnLine, 54*(20): 801–806.
17. Memon J, Sami M, Khan R A, Uddin M. Handwritten Optical Character Recognition (OCR): A Comprehensive Systematic Literature Review (SLR). IEEE Access, 2020, 8: 142642–142668.

18. Cai B. Deep learning Optical Character Recognition in PCB Dark Silk Recognition. 2022. *World Journal of Engineering and Technology, 11*(1): 1–9.
19. Firdaus A L, Kurnia M S, Shafera T, et al. 2021. Implementasi Optical Character Recognition (OCR) Pada Masa Pandemi Covid-19. *JUPITER (Jurnal Penelitian Ilmu dan Teknik Komputer), 13*(2): 188–194.
20. Paul M A, Rani P A J, Sheela J. 2021. Coral Reef Classification Using Improved WLD Feature Extraction with Convolution Neural Network Classification. *Recent Advances in Computer Science and Communications (Formerly: Recent Patents on Computer Science), 14*(8): 2579–2588.